

# Hydrosulfurization Cobalt-based Catalysts Modified by Gold

AM Venezia<sup>\*1</sup>, R Murania<sup>2</sup>, G Pantaleo<sup>2</sup>,  
G Deganello<sup>1,2</sup>

<sup>1</sup> Istituto dei Materiali Nanostrutturati (ISMN-CNR) via  
Ugo La Malfa, 153, Palermo, I- 90146

<sup>2</sup> Dipartimento di Chimica Inorganica ed Analitica  
'Stanislao Cannizzaro', Università di Palermo, Viale  
delle Scienze – Parco d'Orleans, Palermo I-90128

\* Corresponding author

E-mail: venezia@pa.ismn.cnr.it

## Abstract

**Cobalt catalysts supported on amorphous SiO<sub>2</sub> and ordered mesoporous silica (MCM-41) were prepared by incipient wetness impregnation. Gold was added by consecutive impregnation or by co-impregnation. The materials were characterised by XPS, XRD and TPR techniques and evaluated in the hydrosulfurization (HDS) of thiophene in order to investigate the effect of the noble metal on the structure and on the catalytic behaviour of the supported cobalt. Co/MCM-41 exhibited higher HDS activity and higher stability than the Co/SiO<sub>2</sub>. Moreover, in contrast to silica case, the gold impregnated MCM-41, produced an enhancement of the cobalt catalytic activity, and this is likely to be related to an increased cobalt reducibility. Both the support and the addition of gold improve the cobalt dispersion.**

## Introduction

The use of gold in catalysis has increased enormously in the last 15 years, following the discovery by Haruta et al. of the high activity of supported gold catalysts for the low temperature oxidation of CO (1). Depending on the catalytic reaction, gold behaves as the active site or acts as a catalyst promoter. Oxidation of CO and the epoxidation of propene are examples of the direct involvement of gold species as active sites (2,3) whereas hydrogenation and hydrodechlorination are typical cases in which promotion of the active metal (Pd) by gold is found (4,5). Recently, some interesting results were obtained in our laboratory concerning the effect of gold on silica-supported palladium catalysts for hydrosulfurization (6,7). In mild conditions, at atmospheric pressure, gold alone was catalytically inert, but when combined with palladium in a bimetallic catalyst, it acted as a structure modifier by decreasing, through alloying, the size of the active Pd ensemble. Moreover, gold inhibited the formation of the less active Pd<sub>4</sub>S. As a result, an enhanced catalyst activity and sulfur tolerance in the HDS of thiophene was observed (6). Under more severe conditions, such as high hydrogen pressure, the gold catalyst was more active than the palladium catalyst, and in the bimetallic catalyst it worked in synergy with palladium. In the latter case, in addition to an increased dibenzothiophene conversion, an enhanced selectivity towards the biphenyl formation rather than the hydrogenated cyclohexylbenzene was observed (7). The comparison of the results obtained under the two different sets of experimental conditions suggested, as a possible mechanism for the HDS, attachment of the substrate to the gold sites followed by C-S rupture activated by the hydrogen.

Hydrosulfurization catalysis is still a major challenge for the petroleum industry, and the objective for the present study was to build on the conclusions of the results summarized above by investigating the effect of gold on the hydrosulfurization activity of cobalt catalysts. Since high surface area materials, such as MCM-41, have been recently reported as promising supports for hydrotreatment reactions (8,9) Co and AuCo catalysts on MCM-41 are prepared and compared with corresponding catalysts supported on amorphous SiO<sub>2</sub>. The materials are characterised by X-ray photoelectron spectroscopy (XPS), X-ray diffraction (XRD) and temperature programmed reduction (TPR) techniques. The catalytic behaviour is evaluated in the HDS of thiophene.

## Experimental

The MCM-41 was prepared using the hydrothermal method described by J. Choma et al. (10). Attainment of the ordered mesoporous structure was confirmed by the XRD pattern showing the typical reflection at  $2\theta \approx 2^\circ$  and by the typical type IV N<sub>2</sub> adsorption-desorption isotherm (9, 11). The catalysts, on SiO<sub>2</sub> (Merck; SSA=316 m<sup>2</sup>/g; d<sub>p</sub> = 5 nm) and on the MCM-41 (SSA=810 m<sup>2</sup>/g; d<sub>p</sub> = 2.6 nm) containing 5 wt%

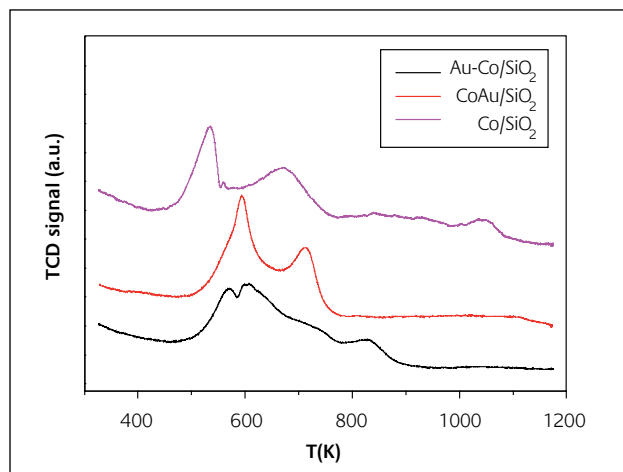


**Figure 1 (a)**

TPR pattern of a) Co/SiO<sub>2</sub> and differently gold promoted Co/SiO<sub>2</sub>

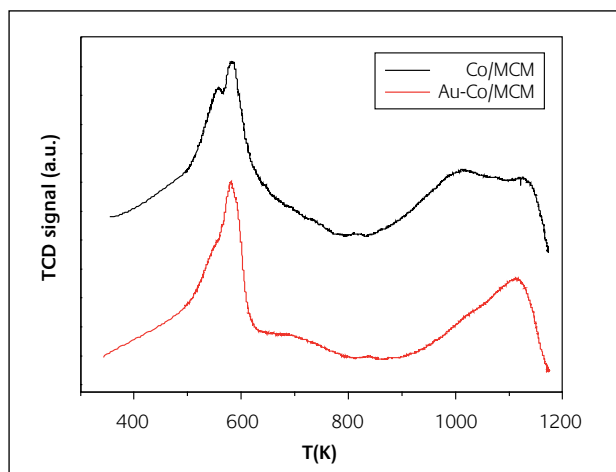


**Figure 1 (b)**

b) Co/MCM-41 and Au-Co/MCM-41 catalyst

Co, were prepared by incipient wetness impregnation of the supports with an aqueous solution of Co(NO<sub>3</sub>)<sub>2</sub>·6H<sub>2</sub>O followed by 2 h drying at 393 K and overnight calcination at 673 K. Gold (1 wt%) was added using two procedures. The first consisted of co-impregnation of the supports with the aqueous solutions of Co(NO<sub>3</sub>)<sub>2</sub>·6H<sub>2</sub>O and HAuCl<sub>4</sub> followed by drying and calcination. The second method involved two consecutive impregnations of the supports. The first impregnation with gold salt solution followed by drying at 393K and calcination at 673 K. Then, the second impregnation with cobalt salt solution as in the former procedure. The sample notation distinguishes between the co-impregnated and the successive impregnation as CoAu/support and Au-Co/support respectively.

X-ray diffraction measurements for the structure determination were carried out with a Philips vertical goniometer using Ni-filtered Cu K $\alpha$  radiation. A proportional counter and 0.05° step size in 2 $\theta$  were used. The assignment of the various crystalline phases was based on the JPDFS powder diffraction file cards (12). The specific surface area (BET) and the pore size distributions were obtained using a Carlo Erba Sorptomat 1900 instrument (13). X-ray photoelectron spectroscopy analyses were performed with a

VG Microtech ESCA 3000 Multilab. The spectra were excited by the unmonochromatised Al K $\alpha$  source (1486.6 eV) run at 14 kV and 15 mA. The binding energies were calibrated with respect to C 1s, from adventitious carbon, set at 285.1 eV. Peak resolution and quantitative analysis were performed using the software provided by VG. TPR measurements, in the range of 323 K - 1173 K, were conducted with a Micromeritics AutoChem 2910 Automated Catalyst Characterization System, equipped with a thermal conductivity detector (TCD). The HDS of thiophene was carried out in a plug-flow microreactor and according to the procedure described previously (6,7). The samples were sulfided in situ with a mixture of 10 vol % H<sub>2</sub>S/H<sub>2</sub>, at 50 ml/min, at 673 K for 2h (6). After purging with nitrogen, the HDS of thiophene was carried out at 613 K with 5.3 vol% thiophene in H<sub>2</sub> and WHSV = 7500 h<sup>-1</sup>. The reaction products were analysed by on-line gas chromatography (Carlo Erba GC 8340). The first-order rate constant for HDS ( $k_{HDS}$ ) was calculated using the equation:  $k_{HDS} = -\ln(1-x)/\tau$ , where  $x$  is the fractional conversion at the steady state conditions, reached after 8h on stream, and  $\tau$  is the space time given by the mass of the catalysts (g) divided by the volumetric reagent gas flow  $F_0$  (ml s<sup>-1</sup>). The percentage of initial deactivation, defined as %  $d = 100 (x_i - x_f)/x_i$  with  $x_i$  and  $x_f$  being the conversion at the

**Table 1**

Specific surface area (BET), average pore diameters,  $d_p$ , and mean crystallite size of Co<sub>3</sub>O<sub>4</sub> and Au phases of cobalt and gold promoted cobalt catalysts after calcination

Sample	SSA (m <sup>2</sup> /g)	$d_p$ (nm)	$d_{Co_3O_4}$ (nm)	$d_{Au}$ (nm)
Co/SiO <sub>2</sub>	276	5	15	
Au-Co/SiO <sub>2</sub>	285	5	13	60
CoAu/SiO <sub>2</sub>	305	5	11	28
Co/MCM-41	632	2.6	9	
Au-Co/MCM-41	698	2.6	5(70%);24 (30%)	37
CoAu/MCM-41	692	2.8	n.d.*	n.d.*

\*n.d. not determined

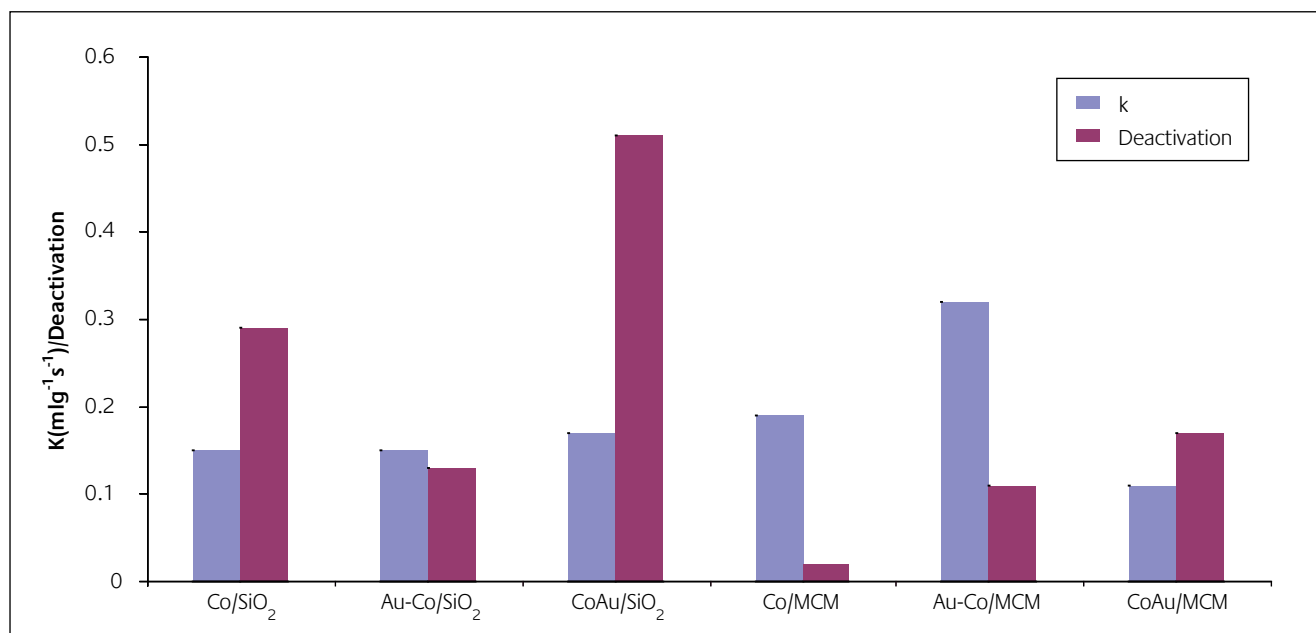


**Figure 2**  
Variation of thiophene HDS rate constant and deactivation with catalyst formulation

initial and steady conditions (after 8 h) respectively was calculated.

## Results and discussion

BET surface areas, average pore diameters and XRD derived sizes of  $\text{Co}_3\text{O}_4$  crystallites and metallic gold particles of the promoted and unpromoted catalysts are listed in Table 1. The surface area of the catalysts supported on MCM-41 are significantly higher with respect to the silica catalysts. It is worth noticing that the gold-containing catalysts have larger areas as compared to the cobalt-only catalysts. With respect to the silica supported catalysts,  $\text{Co}_3\text{O}_4$  particles supported on the large area support, MCM-41, have smaller size. It is worth noticing the bimodal distribution obtained when cobalt is supported over the support first impregnated with gold.

In Figure 1 the TPR profiles of the  $\text{SiO}_2$  and MCM-41 supported catalysts are given. The reduction curve of Co supported on silica is characterised by two large peaks. According to the literature, on unsupported  $\text{Co}_3\text{O}_4$  (14) the

reduction process occurs in two steps, a lower temperature reduction of  $\text{Co}^{3+}$  to  $\text{Co}^{2+}$  and a slightly higher temperature reduction of  $\text{Co}^{2+}$  to  $\text{Co}^0$ . The small peak above 1100 K is attributed to the high temperature driven formation of  $\text{CoOx-SiO}_2$  species (15). Addition of gold modifies the reduction pattern in a way related to the metal introduction method. However, due to a variety of effects, such as particle size, morphology and some degree of heterogeneity of the mixed  $\text{Co}_3\text{O}_4$ -Au system, the shape of the peaks is not well defined (15-17). The TPR patterns of the two better performing MCM-41 supported catalysts (Figure 2b) have two major features, one at  $\sim 573$  K and the other above 900 K. The presence of a large reduction peak at such a high temperature indicates that Co interacts more strongly with MCM-41 than with  $\text{SiO}_2$  in accord with the literature (10). Adding gold in this case produces a slight decrease of the high temperature peak. Such effect, although to a larger extent was also observed with other noble metals, such as Pt and Rh (18).

The catalytic results, in terms of rate constant and percentage of initial deactivation, are summarised in Figure 2. With the  $\text{SiO}_2$ -supported catalysts, the first impregnation with gold has a negligible effect on the cobalt activity but

**Table 2**  
XPS data of the calcined and sulfided samples. The percentages of reduced Co and  $\text{Co}^{2+}$  are given in parentheses

Sample	Co 2p <sub>3/2</sub>		Co/Si	
	calc.	sulf.	calc.	sulf.
Co/SiO <sub>2</sub>	780.5	778.5 (33); 781.6 (67)	0.01	0.01
Au-Co/SiO <sub>2</sub>	780.5	778.5 (30); 781.5 (70)	0.02	0.02
CoAu/SiO <sub>2</sub>	780.7	778.5 (29); 781.9 (71)	0.02	0.02
Co/MCM-41	780.5	779.1 (20); 781.5 (80)	0.01	0.04
Au-Co/MCM-41	780.7	778.7(30); 781.7 (70)	0.02	0.02

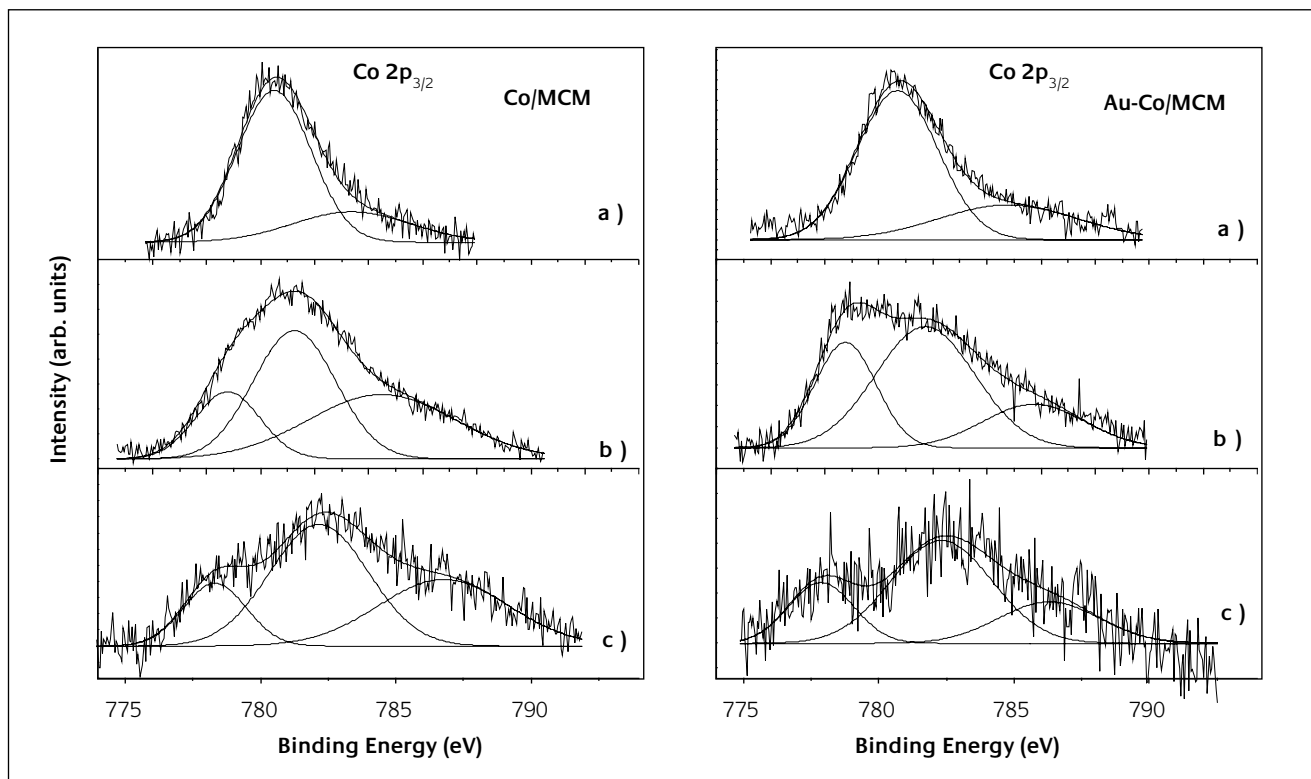


**Figure 3**

*Co 2p<sub>3/2</sub> photoelectron spectra of Co/MCM-41 and Au-Co/MCM-41 a) as received; b) after pre-treatment with H<sub>2</sub>/H<sub>2</sub>S, c) after HDS reaction*

it has a positive effect on the initial deactivation. In the case of co-impregnated Au and Co, an increase in activity with a high initial deactivation is observed. It should be kept in mind that such deactivation, although a negative consideration for a commercial application, corresponds to a large initial activity which is also related to the presence of gold. The use of the MCM-41 improves both the activity and the initial stability of the cobalt catalyst. Most important, on this support, first impregnated with gold, the activity increases significantly.

In order to evaluate the surface modification of the catalysts due to different treatments, the XPS data are listed in Table 2 in terms of Co 2p<sub>3/2</sub> binding energies and of the Co/Si atomic ratios for the cobalt catalysts after calcination and after sulfidation. For all catalysts, the Au 4f<sub>7/2</sub> binding energy of 85.2 eV, typical of metallic gold, was found (6). The Co 2p<sub>3/2</sub> energy value of 780.6 eV ± 0.1 of the calcined samples is intermediate between the values for Co<sup>3+</sup> and the Co<sup>2+</sup> species (19). In agreement with the XRD data, the spectra of the oxidised catalysts are attributed to the Co<sub>3</sub>O<sub>4</sub> phase and, according to the increased atomic ratio Co/Si, the presence of gold favours the surface dispersion of the cobalt phase. The Co 2p<sub>3/2</sub> photoelectron spectra of the better performing catalysts, Co/MCM-41 and Au-Co/MCM-41, after different treatments, are shown in Figure 3. The spectra of the calcined catalysts (Figure 3a) are characterised by a main component and a small satellite (shake up) peak attributed to Co<sub>3</sub>O<sub>4</sub>. After pre-treatment in H<sub>2</sub>/H<sub>2</sub>S, as shown in Figure 3b and as listed in Table 2 for all the catalysts, two components, one at 778.8 eV ± 0.3 and the other at

781.7 eV ± 0.2 with an increased shake up feature, appear. The peak at low energy is due to a reduced cobalt species, either a Co<sub>9</sub>S<sub>8</sub> or cobalt metal, being indistinguishable (20). The peak at 781.7 eV with the shake up at ~786.5 eV is attributed to Co<sup>2+</sup>. As shown in the figure, the gold-containing sample as compared to the only cobalt sample exhibits an increase of the intensity of the reduced Co 2p component relatively to the oxidised Co 2p species. This effect, ascribable to the gold promoted cobalt reducibility, along with the increased cobalt dispersion, can explain the larger activity of the Au-Co/MCM-41 catalyst. As shown in Figure 3c, after the reaction, a deterioration of the Co 2p signal occurs. The corresponding decrease of the Co 2p/Si 2p and Au 4f/Si 2p intensity ratios are probably due to carbon deposition in accord with a small increase of the C1s signal.

## Conclusions

According to the structural and surface characterization results, the higher activity of the Au-Co/MCM-41 catalyst, as compared to the analogous SiO<sub>2</sub>-supported catalyst, is due to the better cobalt dispersion over the larger surface area support. The impregnation of this support with gold, before adding cobalt, allows for a further increase of the cobalt dispersion and of most importance, it favours the reducibility of Co upon treatment with H<sub>2</sub>/H<sub>2</sub>S. On SiO<sub>2</sub>, where the weak interaction between cobalt and the support favours a higher Co sulfidation, the effect of gold is negligible.

Therefore, the combination of the different support and of gold addition, contributes to the enhancement of the HDS activity of the consecutively impregnated Au-Co/MCM-41 catalyst. These positive effects will be further explored in order to enhance them and to find ways of reducing the initial catalyst deactivation.

## Acknowledgements

Support by European Community, Network of Excellence (NoE) IDECAT (Integrated Design of Catalytic Nanomaterials for Sustainable Production) and by COST D36/0003/06 is acknowledged.

## About the authors



**Dr. AM Venezia** is director of research at the ISMN in Palermo. She worked as postdoctoral fellow at the Material Research Laboratory in Urbana, Illinois and she received her PhD from the University of Alberta, Canada in 1984.



**G Deganello**, is professor of inorganic chemistry at the University of Palermo, he is the head of the ISMN Division in Palermo.



**G Pantaleo** is a chemical engineer, working in the group as the expert in gas-phase reactions and catalyst characterization by TPR.



**R Murania** is a graduate student in chemistry at the University of Palermo.

## References

- 1 M. Haruta, N. Yamada, T. Kobayashi and S. Iijima, *J. Catal.*, 1989, **115**, 301
- 2 G. C. Bond and D. T. Thompson, *Catal. Rev.-Sci. Eng.*, 1999, **41**, 319
- 3 T. Hayashi, K. Tanaka and M. Haruta, *J. Catal.*, 1998, **178**, 566
- 4 G. C. Bond and A. F. Rawle, *J. Mol. Catal. A*, 1996, **109**, 261
- 5 M. Bonarowska, J. Pielaszek, W. Juszczyk and Z. Karpinski, *J. Catal.*, 2000, **195**, 304
- 6 A. M. Venezia, V. La Parola, V. Nicoli, and G. Deganello, *J. Catal.*, 2002, **212**, 5
- 7 A. M. Venezia, V. La Parola, G. Deganello, B. Pawelec and J.L.G. Fierro, *J. Catal.*, 2003, **215**, 317
- 8 A. Corma, A. Martinez and V. Martinez-Soria, *J. Catal.*, 1997, **169**, 480
- 9 A. Wang, Y. Wang, T. Kabe, Y. Chen, A. Ishihara and W. Quian, *J. Catal.*, 2001, **199**, 19
- 10 J. Choma, S. Pikus and M. Jaroniec, *Appl. Surf. Sci.*, 2005, **252**, 562
- 11 J. Panpranot, J. G. Goodwin Jr. and A. Sayari, *Catal. Today*, 2002, **77**, 269
- 12 JCPDS Powder Diffraction File, Int. Centre for Diffraction Data, Swarthmore
- 13 S. J. Gregg and K. S. Sing, Adsorption, Surface Area and Porosity, 2nd ed., Academic Press, San Diego, 1982
- 14 B. A. Sexton, A. E. Hughes and T. Turney, *J. Catal.*, 1986, **97**, 390
- 15 G. Jacobs, T. K. Das, Y. Zhang, J. Li, G. Racollet, and B. H. Davis, *Appl. Catal. A*, 2002, **233**, 263
- 16 M. Voß, D. Borgmann and G. Wendler, *J. Catal.*, 2002, **212**, 10
- 17 L. B. Backman, A. Rautiaien, M. Lindblad, O. Jylha and A. O. I. Krause, *Appl. Catal. A*, 2001, **208**, 223
- 18 M. M. Hossain, M. A. Al-Saleh, M. A. Shalabi, T. Kimura and T. Inui, *Appl. Catal. A*, 2004, **274**, 43
- 19 M. A. Stranick, M. Houalla and D. M. Hercules, *J. Catal.*, 1987, **103**, 151
- 20 Y. Okamoto, T. Imanaka, and S. Teranishi, *J. Catal.*, 1980, **85**, 448